

# Lanthanide(III) Complexes of Bis(phosphonate) Monoamide Analogues of DOTA: Bone-Seeking Agents for Imaging and Therapy

Tomáš Vitha,<sup>†,§</sup> Vojtěch Kubíček,<sup>§</sup> Petr Hermann,<sup>§</sup> Luce Vander Elst,<sup>‡</sup> Robert N. Muller,<sup>‡</sup> Zvonimir I. Kolar,<sup>||</sup> Hubert T. Wolterbeek,<sup>||</sup> Wouter A.P. Breeman,<sup>⊥</sup> Ivan Lukeš,<sup>\*,§</sup> and Joop A. Peters<sup>\*,†</sup>

*Biocatalysis and Organic Chemistry, Department of Biotechnology, Delft University of Technology, Julianalaan 136, 2628 BL Delft, The Netherlands, Department of Inorganic Chemistry, Charles University, Hlavova 8, 128 40 Prague, Czech Republic, Department of General, Organic and Biomedical Chemistry, NMR and Molecular Imaging Laboratory, University of Mons Hainaut, B-7000, Mons, Belgium, Department of Radiation, Radionuclides and Reactors, Faculty of Applied Sciences, Delft University of Technology, 2629 JB Delft, The Netherlands, and Department of Nuclear Medicine, Erasmus MC, 3015 GD Rotterdam, The Netherlands*

Received October 10, 2007

Lanthanide complexes of DOTA derivatives **2a** (BPAMD) and **2b** (BPAPD), having a monoamide pendant arm with a bis(phosphonate) moiety, were comparatively tested for application in MRI, radiotherapy, and bone pain palliation. <sup>1</sup>H, <sup>31</sup>P, and <sup>17</sup>O NMR spectroscopy show that they are nine-coordinated, with one water molecule in the first coordination sphere of the Ln(III) ion. The bis(phosphonate) moieties are not coordinated to the lanthanide and predominantly mono- and diprotonated at physiological pH. The parameters governing the longitudinal relaxivities of the Gd complexes are similar to those of other monoamides of DOTA reported in the literature. Upon adsorption on hydroxyapatite, the relaxivities at 20 MHz and 25 °C of Gd-**2a** and Gd-**2b** were 22.1 and 11 s<sup>-1</sup> mM<sup>-1</sup>, respectively. An in vivo  $\gamma$ -ray imaging study showed that the <sup>177</sup>Lu complexes of **2a** and **2b** have a high affinity for bones, particularly for growth plates and teeth with a prolonged retention.

## Introduction

A major field of applications of MRI contrast agents (CAs<sup>a</sup>) is in diagnosis of carcinoma in soft tissues.<sup>1–4</sup> However, it is known that metastasis of almost all types of cancer may affect bones.<sup>5</sup> A variety of other diseases like cerebral and myocardial infarcts cause abnormal calcium accumulations in soft tissues as well.<sup>6</sup> Curiously, the presently applied imaging techniques for calcified tissues are solely based on radiodiagnostic methods, and there is currently no MRI alternative available in clinical use.

Radiodiagnosis relies on  $\gamma$ -ray scanning using <sup>99m</sup>Tc complexes with simple geminal bis(phosphonate) ligands, such as methanediphosphonic acid (MDP) and 1-hydroxyethane-1,1-diphosphonic acid (HEDP).<sup>7</sup> The bis(phosphonic acid) group exhibits a high affinity for the bone surface both in the free form and in the form of metal complexes. It is adsorbed

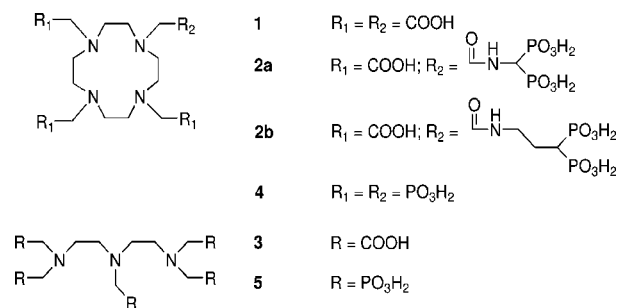


**Figure 1.** Structures of ligands discussed.

preferentially to the active parts of bones such as areas of natural growing and those undergoing some pathological changes.<sup>8</sup>

In efforts to develop bone-targeted CAs for MRI, phosphonate and/or bis(phosphonate) moieties have also been exploited to deliver the CA to the area of interest.<sup>6,9–15</sup> For example, the Ln(III) complexes of phosphonate analogues of 1,4,7,10-tetraazacyclododecane-1,4,7,10-tetraacetic acid (DOTA, **1**) and diethylenetriamine-*N,N,N',N'',N'''*-pentaacetic acid (DTPA, **3**; i.e., compounds **4** and **5**; Figure 1) have been shown to exhibit a rather strong adsorption on hydroxyapatite (HA), a model of bone surface.<sup>9,10</sup> These complexes, however, have major drawbacks; the relaxivity of Gd-**4** quenches upon adsorption to HA due to expulsion of second-sphere water molecules from the vicinity of the complex,<sup>9</sup> whereas Ln-**5** shows critical loss of complex stability upon interaction with HA due to extensive interaction with its surface.<sup>10</sup> Another candidate, a bis(phosphonate)-modified DTPA, showed a low in vitro stability.<sup>12</sup> Recently, we achieved rather promising results by attaching a bis(phosphonate) via an amide moiety to DOTA (compound **2a**; Figure 1).<sup>15</sup> An in vitro study showed swift, very strong, and reversible adsorption of the Ln(III) complexes of **2a** on HA. Furthermore, the relaxivity of Gd-**2a** appeared to be rather high, and no quenching occurred upon adsorption on HA; on

\* To whom correspondence should be addressed: Tel.: +31152785892 (J.A.P.); +420-221951259 (I.L.). Fax: +31152781415 (J.A.P.); +420-221951253 (I.L.). E-mail: j.a.peters@tudelft.nl (J.A.P.); lukes@natur.cuni.cz (I.L.).

<sup>†</sup> Biocatalysis and Organic Chemistry, Delft University of Technology.

<sup>§</sup> Charles University.

<sup>‡</sup> University of Mons Hainaut.

<sup>||</sup> Department of Radiation, Radionuclides and Reactors, Faculty of Applied Sciences, Delft University of Technology.

<sup>⊥</sup> Erasmus MC.

<sup>a</sup> Abbreviations: BPAMD, (4-[[bis-(phosphonomethyl)carbamoyl]methyl]-7,10-bis(carboxymethyl)-1,4,7,10-tetraazacyclododec-1-yl)acetic acid; BPAPD, (4-[[bis(phosphonopropyl)carbamoyl]methyl]-7,10-bis(carboxymethyl)-1,4,7,10-tetraazacyclododec-1-yl)acetic acid; CA, contrast agent; DOTA, 1,4,7,10-tetraazacyclododecane-1,4,7,10-tetraacetate; DO3A, 1,4,7,10-tetraazacyclododecane-1,4,7-triacetic acid; DTPA, diethylenetriamine-*N,N,N',N'',N'''*-pentaacetic acid; HA, hydroxyapatite; HEDP, 1-hydroxyethane-1,1-diphosphonic acid; ID, injected dose; LIS, lanthanide-induced shift; MDP, methanediphosphonic acid; NMRD, nuclear magnetic resonance dispersion; R<sub>1</sub>, longitudinal relaxation rate; R<sub>2</sub>, transversal relaxation rate; SA, square-antiprismatic; TSA, twisted square-antiprismatic.

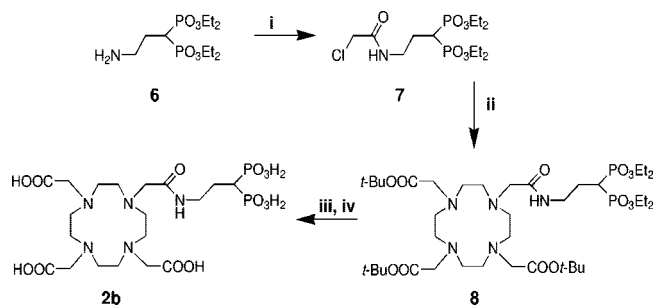


**Figure 2.** Synthesis of the bone targeting ligand **2b**. (i)  $\text{ClCH}_2\text{C}(\text{O})\text{Cl}$ , acetonitrile,  $\text{K}_2\text{CO}_3$ ,  $-50\text{ }^\circ\text{C}$  to RT, 24 h; (ii)  $t\text{-Bu}_3\text{DO3A}$ , acetonitrile,  $\text{K}_2\text{CO}_3$ , RT, 4 d; (iii)  $\text{CF}_3\text{COOH}/\text{CH}_2\text{Cl}_2$  (1:1), reflux, 12 h; (iv) 30% HBr in dry AcOH, RT, 24 h.

the contrary, the relaxivity increased upon adsorption due to the immobilization of the complex.<sup>15</sup>

Now, we extended our research to lanthanide(III) complexes of a ligand with a somewhat longer linker between the DOTA unit and the bis(phosphonate) function: (4-[[bis(phosphonopropyl)carbamoyl]methyl]-7,10-bis(carboxymethyl)-1,4,7,10-tetraazacyclododec-1-yl)acetic acid (**2b**, see Figure 1). Here, we report on its synthesis, the relaxivity of its Ln(III) complexes and on in vivo studies with Ln(III) complexes of both **2a** and **2b**.

As a result of the shielding of their 4*f* valence electrons by the 5*s* and 5*p* electrons, the 15 Ln(III) ions have very similar chemical behavior and the various Ln(III) complexes of a particular ligand are generally almost isostructural. In the present study, we exploited this isostructurality by performing each of the various physicochemical and in vivo studies with the use of the most effective Ln(III) ion for that particular technique. It may be assumed that the results give a good picture for the properties of the complexes of all other Ln(III) ions. For example, a comparison of the pharmacokinetics and biodistribution in rats was determined by  $\gamma$ -ray imaging using the <sup>177</sup>Lu complexes of **2a** and **2b**. The adsorption of both compounds on HA appeared to be very strong;<sup>15,16</sup> these complexes are bound as a monomolecular layer on the surface of HA. The affinity constants for Tb-**2a** and Tb-**2b** for HA are  $2.1 \times 10^5$  and  $2.2 \times 10^4 \text{ L mol}^{-1}$ , respectively.<sup>16</sup> In the latter studies <sup>160</sup>Tb was the selected Ln(III) ion because of its long half-life time (72.1 days).

## Results and Discussion

**Syntheses.** The pendant arm (**7**) of ligand **2b** was prepared in 89% yield by the reaction of chloroacetyl chloride with tetraethyl 3-aminopropyl-1,1-bis(phosphonate) (**6**; see Figure 2). Alkylation of the tris(*t*-butylester) of DO3A with this bis(phosphonate) followed by a two-step de-esterification procedure of the resulting ester (**8**) and purification by repeated column chromatography on a weak cation exchange resin gave the desired **2b** in 30% yield. The rather low yield is caused by degradation during the de-esterification steps and by a low efficiency of the chromatographic purification. The Ln(III) complexes of **2b** were prepared by heating of aqueous solutions of the lanthanide(III) chloride or nitrate in question with the ligand in 10% excess at pH 8–9 followed by adjustment of the pH. The synthesis of ligand **2a** has been described previously.<sup>15</sup>

**The Structure of Ln-2a and Ln-2b in Aqueous Solution.** Because bis(phosphonates) have a strong affinity for Ca(II), they may have an even stronger affinity for Ln(III) ions. Therefore, it is important to establish that the Ln(III) ion in its complexes of **2a** and **2b** is coordinated in the macrocyclic cavity and that

**Table 1.** Amount of the Diastereoisomer *m* (TSA, mol %) in Solutions of Lanthanide(III) Complexes of some DOTA Derivatives (pH 7, 25 °C)

Ln	<b>1</b> <sup>a</sup>	<b>2a</b> <sup>b</sup>	<b>2b</b> <sup>c</sup>
Eu	22	18	19
Yb	7	0	7

<sup>a</sup> Ref 17. <sup>b</sup> Ref 15. <sup>c</sup> This work.

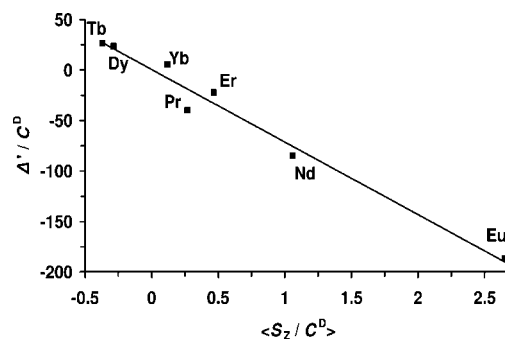


**Figure 3.** Plot of  $\Delta'/C^D$  vs  $\langle S_z \rangle / C^D$  for the <sup>17</sup>O water shifts of Ln-**2b** (pH 7, 76 °C).

the phosphonate functions in these complexes are not involved in the coordination of the Ln(III) ion.

The <sup>1</sup>H NMR spectra of the Eu(III) and Yb(III) complexes are very similar to those of the corresponding DOTA complexes (see Supporting Information, Figure S1). The number of resonances in the spectra of the Ln-**2a**<sup>15</sup> and Ln-**2b** complexes, however, is larger due to the lower symmetry of these complexes as compared to Ln-DOTA. Typically, two sets of peaks were observed, of which the lanthanide-induced chemical shifts of one of the sets were larger than those of the other one. Lanthanide(III) complexes of DOTA-like ligands are known to occur in solution as a mixture of two diastereomeric forms, which differ in the mutual orientation of the “nitrogen” and “oxygen” planes of the coordination polyhedron: the square-antiprismatic (SA, usually labeled *M*) and twisted square-antiprismatic forms (TSA, usually labeled *m*).<sup>17</sup> The ratio of *m*/*M* commonly changes along the lanthanide series. The ratios of the intensities of the two sets of spectra of Ln-**2a** and Ln-**2b** (see Table 1) are similar to those reported for Ln-DOTA complexes.<sup>18,19</sup> The great similarity of the <sup>1</sup>H NMR spectra of these compounds with those of the corresponding Ln-DOTA complexes suggests that the Ln(III) ions are bound in a similar fashion.

The number of water molecules in the first coordination sphere of the Ln(III) ion in Ln-**2b** was evaluated with the use of the lanthanide-induced <sup>17</sup>O NMR chemical shifts (Ln = Pr, Nd, Eu, Tb, Dy, Er, Yb). These shifts were extrapolated to a molar ratio of Ln-complex to water of 1 and then corrected for the diamagnetic contribution by subtraction of the shifts for the corresponding diamagnetic La(III) complex. A plot of  $\Delta'/C^D$  versus  $\langle S_z \rangle / C^D$  for Ln-**2b** gives a perfect straight line (correlation coefficient > 0.97, see Figure 3). Here  $\Delta'$  is the extrapolated and corrected lanthanide-induced shift and  $C^D$  and  $\langle S_z \rangle$  are parameters, which are dependent on the lanthanide and which are tabulated in the literature.<sup>20–24</sup> The linearity in this plot indicates that the hydration number (*q*) of the complexes concerned is constant along the Ln(III) series. The slope of this line (*F*) is  $-71.9$ . Previously, it has been shown that  $F = q \times (-70 \pm 11)$ <sup>25–27</sup> and, therefore, it can be concluded that Ln-**2b** complexes have one coordinated water molecule in the first coordination sphere of all Ln(III) ions. Previously, we have reached a similar conclusion for Ln-**2a**.<sup>15</sup> Therefore, it is very

**Table 2.** pK<sub>a</sub> and logβ values of the bis(phosphonate) moieties of Yb-2a and Yb-2b in water (0.15 M)<sup>a</sup>

species	Yb-2a		Yb-2b		H <sub>4</sub> aca <sup>b</sup>	
	logβ	pK <sub>a</sub>	logβ	pK <sub>a</sub>	logβ	pK <sub>a</sub>
H <sub>2</sub> L	15.64(14)	1.8	23.35(24)	1.6	25.34(8)	1.4
H <sub>3</sub> L <sup>-</sup>	13.89(11)	4.9	21.76(11)	4.1	23.98(7)	5.8
H <sub>2</sub> L <sup>2-</sup>	8.97(6)	9.0	17.63(11)	6.7	18.22(6)	7.5
HL <sup>3-</sup>		>13	10.94(3)	10.9	10.73(4)	10.7

<sup>a</sup> As determined from <sup>31</sup>P and/or <sup>1</sup>H NMR titration data in comparison with those for H<sub>4</sub>aca (acetamidomethyl-bis(phosphonic acid; 25 °C)). <sup>b</sup> Ref 30.

unlikely that the bis(phosphonate) group is coordinated to the Ln(III) ion as well in these complexes.

Further support for the noninvolvement of the bis(phosphonate) function in the coordination of the Ln(III) ion was obtained from the distances of the bis(phosphonate) function from the Ln(III) ion, as determined by means of lanthanide-induced longitudinal relaxation rate enhancements. The two <sup>31</sup>P resonances of Dy-2a were well separated, so the longitudinal relaxation rates of these nuclei were measured, and with the use of an equation taking into account both the dipolar and the Curie relaxation,<sup>25</sup> the distances between the Dy(III) ion and the two phosphorus atoms were estimated to be 6.5 and 6.2 Å, respectively.<sup>15</sup> These distances are too long for binding of the phosphonate groups to the Dy(III) ion. In the NMR spectra of the Ln-2b complexes, the <sup>31</sup>P resonances were coinciding at the chemical shift of this resonance in the free ligand (20 ppm). Therefore, for this system, the R<sub>1</sub> value of the <sup>1</sup>H resonance for the -CH(PO<sub>3</sub>H<sub>2</sub>)<sub>2</sub> proton in Yb-2b (25.3 s<sup>-1</sup>), which was not overlapping with any other resonance, was used. From this relaxation rate enhancement, the distance of this proton to the central Yb(III) ion was calculated to be 5.0 Å. An inspection of molecular models then suggests that the bis(phosphonate) pendant arm is in the proximity of the macrocyclic part of the molecule (Figure S2). This can be ascribed to the involvement of the phosphonate groups in intramolecular hydrogen bond formation. However, a direct coordination of the bis(phosphonic acid) group to the metal ion can be excluded (<sup>31</sup>P NMR spectra show signals only around 20 ppm).

The pK<sub>a</sub> values of bis(phosphonate) moiety in the Yb(III) complex of 2a were determined from NMR titration data of the two nonequivalent <sup>31</sup>P resonances. The pK<sub>a</sub> values of the bis(phosphonate) moiety in Yb-2b were determined using NMR titration data of the -CH(PO<sub>3</sub>H<sub>2</sub>)<sub>2</sub> proton and those of the equivalent <sup>31</sup>P resonances (see Supporting Information, Figure S3). The latter pK<sub>a</sub> values of the bis(phosphonate) moiety obtained for Yb-2b (see Table 2) are in good agreement with data reported commonly for bis(phosphonate) moieties,<sup>28–30</sup> which once again demonstrates that the bis(phosphonate) group in this complex is not coordinated to the Ln(III) ion, because coordination would have resulted in a decrease of the pK<sub>a</sub> values. The values of pK<sub>a3</sub> and pK<sub>a4</sub> for Yb-2a are substantially higher, whereas the latter one is even 3 orders of magnitude higher than the value found for the corresponding acetamide<sup>30</sup> (see Table 2), which suggests that the mono- and diprotonated species are stabilized by rather strong hydrogen bonds between the phosphonate functions and the macrocycle. This is in agreement with the conclusions based on the relaxation rate enhancements (see above).

Therefore, it can be concluded that the Ln-2a and Ln-2b complexes are nine-coordinated with one coordinated water molecule in the first sphere and free bis(phosphonate) moieties, which occur predominantly in the mono- and diprotonated forms at physiological pH.

**Table 3.** Relaxivities of Gd-2a and Gd-2b and the Most Important Parameters Governing It, as Compared To Those of Gd-1 (pH = 7.5, 25 °C)

ligand	τ <sub>M</sub> [μs]	τ <sub>R</sub> [ps]	τ <sub>v</sub> [ps]	Δ <sup>2</sup> [s <sup>-2</sup> /10 <sup>19</sup> ]	r <sub>1</sub> [20 MHz; s <sup>-1</sup> mM <sup>-1</sup> ]
2a <sup>a,b</sup>	1.1 ± 0.2	95 ± 5	22 ± 1	2.6 ± 0.1	5.3
2b <sup>b</sup>	1.1 ± 0.2	86 ± 3	27 ± 1	1.2 ± 0.1	5.0
1 <sup>c</sup>	0.24 ± 0.01	77 ± 4	11 ± 1	1.6 ± 0.1	4.8

<sup>a</sup> The values differ slightly from the previously published ones, which were obtained from a fitting of only the <sup>17</sup>O transversal relaxation rates and the <sup>1</sup>H NMRD profile (ref 15). <sup>b</sup> This work. <sup>c</sup> Ref 32.

### Evaluation of the Relaxivity and the Parameters Governing It

To evaluate the parameters governing the relaxivity of the Gd-2b complex, variable-temperature <sup>17</sup>O longitudinal and transversal relaxation rates (R<sub>1</sub> and R<sub>2</sub>), <sup>17</sup>O chemical shifts of water and a <sup>1</sup>H NMRD profile were measured (see Supporting Information, Figures S4 and S5). These data were fitted simultaneously with a set of equations described previously.<sup>31</sup> The most important parameters are compared with those reported for Gd-2a<sup>15</sup> and Gd-1 in Table 3 (for a full list of parameters, see Supporting Information, Table S1). The value of the residence time of water (τ<sub>M</sub>) in the Gd-2b complex is comparable with that found for Gd-2a and is substantially longer than that of Gd-1.<sup>32</sup> A similar behavior has been observed for other Gd(III) complexes of DOTA, in which one of the carboxylate functions was replaced by an amide function.<sup>33</sup> The rotational correlation times of the various complexes (τ<sub>R</sub>) are in agreement with the generally observed values for complexes of this size. The values of parameters determining the electronic relaxation, the mean square zero-field splitting energy (Δ<sup>2</sup>), and the correlation times of the zero-field splitting modulation (<sup>298</sup>τ<sub>v</sub>) for Gd-2a and Gd-2b are close to those reported for similar ligands (see Table 3). Simulations show that the relaxivity of the complexes upon immobilization (increase of τ<sub>R</sub>) will be limited by the nonoptimal values of τ<sub>M</sub>.

Previously, we have reported the <sup>1</sup>H NMRD profile of Gd-2a adsorbed on HA.<sup>15</sup> This profile could be described as the sum of the contributions coming from the paramagnetic complex and the profile for HA. The latter compound has a high relaxivity at low field,<sup>15</sup> which can be explained by the long correlation time modulation of the dipole–dipole relaxation of the protons. This very long correlation time is due to the adsorption equilibrium of the water molecules on the surface of HA and to their subsequent slow motion. The measurement of the <sup>1</sup>H NMRD profile was performed with a large excess of HA (using 1 mM Gd-2a), and therefore, only a negligible fraction of the HA surface (<4%) was occupied by Gd-2a. Under similar conditions, the profile for Gd-2b did not differ much from that of HA. Therefore, the profile was measured using a ten times higher concentration of the paramagnetic complex. Then, the fraction of the HA surface that is occupied by the complex is no longer negligible. It may be assumed that upon adsorption of a complex, the water molecules on the HA surface will be expelled, and consequently, the paramagnetic contribution cannot be obtained by subtracting the relaxation rates of HA. In this case, the paramagnetic contribution to the <sup>1</sup>H NMRD profile was evaluated by subtracting a fraction of the relaxation rates for HA and iterating the magnitude of that fraction until the low-field part of the resulting <sup>1</sup>H NMRD profile was horizontal up to a Larmor frequency of 1 MHz. This situation was reached when a fraction of 0.34 was applied. The resulting paramagnetic portion of the <sup>1</sup>H NMRD profile is compared with those of Gd-2a and the corresponding “free” complexes in Figure 4. Attempts to fit these profiles using the parameters obtained for the free complexes and varying only τ<sub>R</sub> were



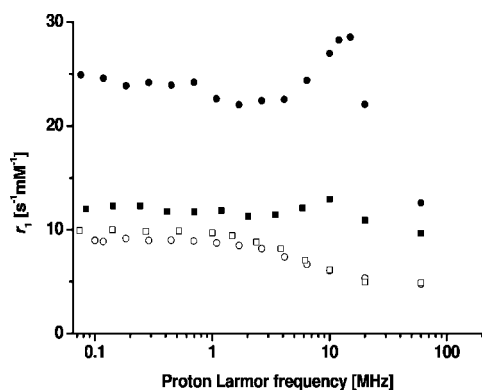


**Figure 4.**  $^1\text{H}$  NMRD profiles of Gd-2a (O) and of Gd-2b (□) and the corresponding profiles of these complexes measured in the presence of HA (• and ■, respectively; pH = 7.5, 25 °C). For conditions, see Experimental Section.

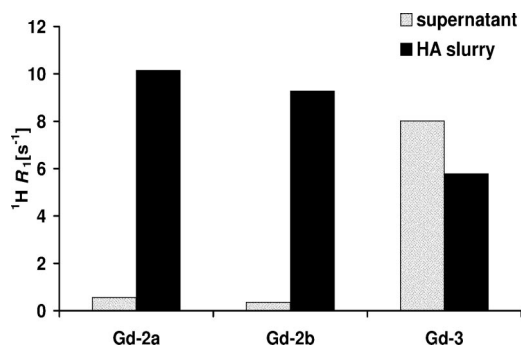


**Figure 5.** Longitudinal  $^1\text{H}$  relaxation rates of the supernatant and the HA layer obtained after sedimentation of an equilibrated aqueous suspension of HA containing Gd-2a, Gd-2b, and Gd-3 in water (pH = 7.5, 25 °C, 300 MHz).

unsuccessful. It can be seen, however, that the relaxivities for Gd-2b adsorbed on HA are rather low, which most likely can be ascribed to the flexibility of the  $\text{C}_3$ -linker between the macrocyclic part of Gd-complex and the bis(phosphonate) moiety. The relaxivities of the Gd-2a complex in the presence of HA are considerably higher, with a pronounced local maximum at about 15 MHz, which is characteristic for compounds with a large  $\tau_R$  value. The relaxivities of this compound at low Larmor frequencies (<1 MHz) are much higher than expected for immobilized Gd-2a. Possibly, this is due to a contribution of water molecules adsorbed on the HA surface, which for this compound are in close proximity to the paramagnetic center. A similar enhancement of the relaxivity has been observed for protein–chelate conjugates.<sup>34</sup>

After standing for a prolonged time (>4 h), both suspensions of Gd-2a and of Gd-2b settled. Measurements of  $^1\text{H}$  relaxation rates indicated that almost all Gd-2a or Gd-2b was in the precipitate (see Figure 5), whereas its amount in the supernatant was negligible, which is in agreement with strong binding of these compounds to HA. A similar experiment performed with Gd-3 showed about equal  $^1\text{H}$  relaxation rates of precipitate and supernatant.<sup>15</sup>

**In Vivo Radioimaging Studies.** Because a free Lu(III) ion has a high affinity for bone, the radioactive complexes were prepared in the presence of a large excess of free ligand (1000 fold). Furthermore, DTPA was added just prior to injection. It has been shown previously that this protocol can remove effectively any free Ln(III) ion and excrete it rapidly via the kidneys.<sup>35,36</sup> Figure 6 represents the dependence of the radioactivity, expressed as % of injected dose (ID), as a function of

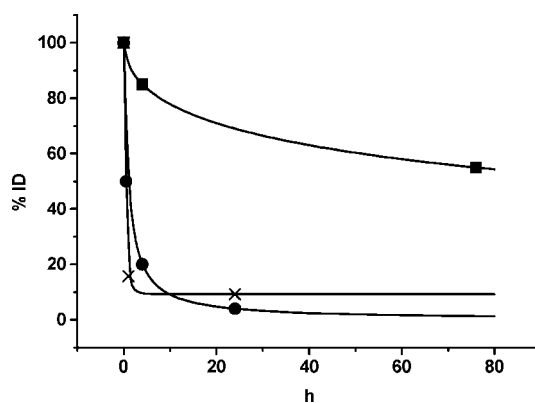


**Figure 6.** Time–activity curves obtained from  $\gamma$ -scintigraphic images obtained after injection of rats with 50  $\mu\text{g}$   $^{177}\text{Lu-3}$  (•), 50  $\mu\text{g}$   $^{177}\text{Lu-2a}$  (■), and 600  $\mu\text{g}$   $^{177}\text{Lu-2a}$  (x). The curves are a guide to the eye.



**Figure 7.**  $\gamma$ -Scintigraphic image of a rat 76 h after injection of  $^{177}\text{Lu-2a}$ .

**Table 4.** Total Body Retention (% ID) of the  $^{177}\text{Lu}$ -Complexes of 2a and 2b upon Injection of 200  $\mu\text{g}$  (75 MBq) in Lewis Rats

time post injection (h)	$^{177}\text{Lu-2a}$	$^{177}\text{Lu-2b}$
1	15.7	14.0
24	9.2	5.3

time after injection of 50  $\mu\text{g}$  of  $^{177}\text{Lu-2a}$  (including an excess of free 2a) in a rat. For comparison, the curve obtained with  $^{177}\text{Lu-3}$  is included in this graph. The bone-targeting complexes undergo an early retention in the skeleton; after the excretion of about 25% of the ID via the kidneys, the radioactivity was exclusively present in the skeleton. Relatively high amounts of radioactivity were observed in the epiphyseal plates and in the teeth. After 72 h, 60% ID of  $^{177}\text{Lu-2a}$  was still present in the skeleton (see Figure 7 and Supporting Information, Figure S6).

A control experiment with  $^{177}\text{Lu-3}$  shows the expected rapid excretion via the kidneys; after 72 h, no radioactivity could be detected anymore, in this case.

The total body retention upon injection of larger amounts of the mixture with  $^{177}\text{Lu-2a}$  (200–600  $\mu\text{g}$ ; 75–80 MBq) was significantly lower (see Table 4), suggesting that, under those conditions, the rate of the uptake in the skeleton compared to the rate of excretion is limiting the body retention. A similar behavior was observed upon administration of  $^{177}\text{Lu-2b}$ , although the total body retention after 24 h was somewhat lower for that complex (see Table 4). The latter is in agreement with

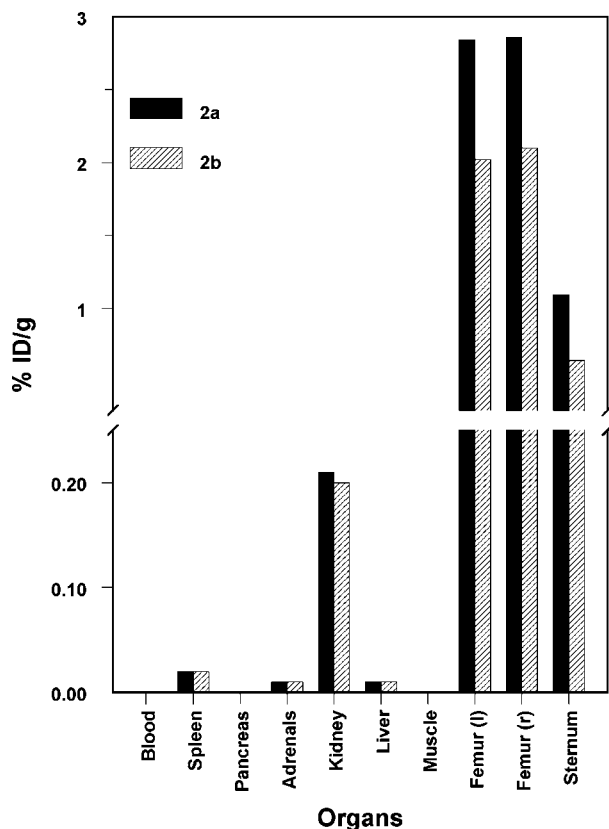


**Figure 8.** Biodistribution of  $^{177}\text{Lu}$ -complexes of **2a** and **2b** in Lewis rat 24 h after injection of 200  $\mu\text{g}$  of compound (complex and excess of free ligand).

the previously observed slightly lower affinity of Ln-**2b** complexes for hydroxyapatite as compared to that of Ln-**2a** complexes.<sup>16</sup>

After 24 and 48 h, the rats were sacrificed to determine the biodistribution. The results are displayed in Figure 8. The high amounts of radioactivity found in the femur and the sternum reflect the high affinity of both complexes for bone. Radiographs of the femurs (see Supporting Information, Figures S7 and S8) confirmed the high accumulation of radioactivity in the epiphyseal plates. The clearance of the complexes occurs mainly via the kidneys, as is demonstrated by the relatively high retention of the radioactivity in the kidneys as compared to that in the liver. A radiograph of the kidneys (see Supporting Information, Figure S9) showed that the radioactivity was present in the cortex (equally distributed over the whole volume of it). Previous studies on  $^{177}\text{LuCl}_3$  showed a very similar behavior; also, that compound has a high affinity for bone and a similar biodistribution as the presently studied compounds, but free  $^{177}\text{Lu(III)}$  ions accumulate in the kidney mainly on the border of the medulla and the cortex.<sup>35,36</sup> It should be noted, however, that  $^{177}\text{LuCl}_3$  is not suitable for bone imaging, because free Ln(III) ions are highly toxic.<sup>37</sup>

## Conclusion

The Gd-complexes of **2a** and **2b** both have one water molecule in the first coordination sphere, which remains bound upon adsorption on HA. Therefore, these compounds are applicable as positive MRI contrast agents.

The Ln(III) complexes of **2a** and **2b** are very selective bone targeting agents. They particularly show high selectivity for newly formed bone and, therefore, they are promising diagnostic agents for bone tumors. The in vivo behaviors of the two

complexes are very similar, but the bone-uptake of the complex of **2b** seems to be slightly slower than that of **2a**. The clearance of  $^{177}\text{Lu}$ -complexes of **2a** and **2b** from the body is mainly via the kidneys, but the clearance from the skeleton is probably too slow for application in MRI. Nevertheless, this compound might be very useful for radiodiagnosis and for bone pain palliation.

## Experimental Section

**Materials.** Commercially available chemicals had synthetic purity and were used as received. Acetonitrile was dried by distillation from  $\text{P}_2\text{O}_5$ . The HBr salt of the tris(*t*-butyl) ester of 1,4,7,10-tetraazacyclododecane-1,4,7-triacetic acid (*t*- $\text{Bu}_3\text{DO}_3\text{A} \cdot \text{HBr}$ ) and tetraethyl 3-aminopropyl-1,1-bis(phosphonate) were synthesized according to published procedures.<sup>38,39</sup> The synthesis of compound **2a** has been described previously.<sup>15</sup> HA was purchased from Fluka (cat. No. 55496); the specific surface area was determined to be  $63 \text{ m}^2 \text{ g}^{-1}$  by  $\text{N}_2$  adsorption using a Quantachrome Autosorb-6B apparatus.  $^{177}\text{LuCl}_3$  was obtained from IDB Baarle Nassau, The Netherlands.

**NMR Spectroscopy.**  $^1\text{H}$  (399.95 and 300.16 MHz),  $^{13}\text{C}$  (100.58 and 75.48 MHz),  $^{31}\text{P}$  (161.9 and 121.5 MHz), and  $^{17}\text{O}$  (54.22 and 40.69 MHz) NMR spectra were recorded on Varian Unity Inova-400 and -300 spectrometers, respectively, using 5 mm sample tubes and, unless stated otherwise, were performed at 25 °C. For the measurements in  $\text{D}_2\text{O}$ , *t*-BuOH was used as an internal standard with the methyl signal referenced to 1.2 ppm ( $^1\text{H}$ ) or 31.2 ppm ( $^{13}\text{C}$ ). The  $^{31}\text{P}$  chemical shifts were measured with respect to 1%  $\text{H}_3\text{PO}_4$  in  $\text{D}_2\text{O}$  as an external reference.  $\text{H}_2\text{O}$  (pH = 7.5) was used as an external chemical shift reference for  $^{17}\text{O}$  resonances. The pH values of the samples were measured at ambient temperature using a Corning 125 pH-meter with a NMR electrode purchased from Aldrich Chemical Co. For the  $^{17}\text{O}$  NMR measurements, 10  $\mu\text{L}$  of  $^{17}\text{O}$ -enriched water (10%  $\text{H}_2^{17}\text{O}$ ) were added into the samples.  $^1\text{H}$  NMR spectra of the samples containing  $\text{H}_2^{17}\text{O}$  were acquired using water suppression by means of presaturation of the water resonance using the decoupler. Lanthanide(III)-induced water  $^{17}\text{O}$  chemical shifts (LIS) were acquired at 76 °C with frequency lock using 73–86 mM samples in  $\text{D}_2\text{O}$  at pH 7. A solution of  $\text{DyCl}_3$  (88 mM) in  $\text{D}_2\text{O}$  was used as a standard for dysprosium(III)-induced water  $^{17}\text{O}$  chemical shift measurements. The  $^{17}\text{O}$  chemical shifts were corrected for the diamagnetic contribution to the LIS by subtraction of the chemical shift of the corresponding diamagnetic La-complex (87 mM, pH = 7). Variable-temperature  $^{17}\text{O}$  NMR measurements of Gd-**2b** (92 mM, pH = 7.5) were performed without frequency lock in the temperature range 4–86 °C.  $^{17}\text{O}$  chemical shifts obtained without frequency lock were corrected for the bulk magnetic shift contribution by measurement of the difference between chemical shifts of  $^1\text{H}$  signals of *t*-BuOH in the paramagnetic sample and in a sample of *t*-BuOH in water (in the absence of the paramagnetic substrate).<sup>40</sup>

The longitudinal ( $R_1$ ) and transversal ( $R_2$ ) relaxation rates were obtained by the inversion–recovery method<sup>41</sup> and the Carr–Purcell–Meiboom–Gil pulse sequence,<sup>42</sup> respectively. The concentration of Ln(III) was determined by bulk magnetic susceptibility measurements.<sup>43</sup>

**Proton NMRD Profiles.**  $^1\text{H}$  NMRD profiles of an aqueous solution of Gd-**2b** (8.3 mM, pH = 7.5) and an HA slurry with adsorbed Gd-**2b** (8.4 mM, pH = 7.5) were measured at 25 °C and a magnetic field range  $4.7 \times 10^{-4}$ –0.35 T using a Stellar SpinMaster FFC-2000 relaxometer. Measurements at 0.47 and 1.42 T were performed with a Bruker Minispec PC-20 and Bruker Minispec mq60, respectively.

**Determination of Dissociation Constants.** The  $\text{pK}_a$  values of the bis(phosphonate) moieties in Yb-**2a** and Yb-**2b** were determined from  $^{31}\text{P}$  NMR titration data, whereas the  $\text{pK}_a$  values of the bis(phosphonate) moieties in Yb-**2b** were determined with the use of  $^{31}\text{P}$  NMR titration data and of  $^1\text{H}$  NMR titration data of the  $-\text{CH}(\text{PO}_3\text{H}_2)_2$  resonance. The pHs of the samples were adjusted using aqueous solutions of HCl and NaOH. The pH values of

samples were measured at ambient temperature using a Corning 125 pH-meter with a NMR electrode purchased from Aldrich Chemical Co. The pH values >12 were calculated from the known concentration of NaOH in the samples.

**Data Evaluation.** The experimental  $^1\text{H}$  NMRD data were fitted simultaneously with  $^{17}\text{O}$  NMR data by means of a least-squares fitting procedure using the Micromath Scientist program version 2.0 (Salt Lake City, UT).<sup>44</sup> The  $pK_a$  values were calculated from pH-NMR titration data using the program package OPIUM.<sup>45</sup> For molecular modeling, HyperChem Release 7.5 for Windows was used.<sup>46</sup>

**Mass Spectrometry.** Mass spectra were recorded on a Bruker Esquire 3000 spectrometer equipped with an electrospray ion source and ion-trap detection. Measurements were carried out in the positive and the negative modes.

**Tetraethyl 3-Chloroacetamidopropyl-1,1-bis(phosphonate) (7).** A solution of tetraethyl 3-aminopropyl-1,1-bis(phosphonate) (**6**; 3.71 g, 11 mmol) in dry acetonitrile (30 mL) was added dropwise into a mixture of chloroacetylchloride (3.75 g, 34 mmol), dry acetonitrile (100 mL), and annealed  $\text{K}_2\text{CO}_3$  (4.4 g, 32 mmol), which was cooled at  $-50^\circ\text{C}$ . The resulting mixture was stirred at RT for 24 h. After filtration of the solids, the volatiles were evaporated under vacuum, yielding 4.1 g (89%) of a colorless viscous oil.  $^1\text{H}$  NMR ( $\text{CDCl}_3$ , 400 MHz):  $\delta$  1.30 (t, 12H,  $-\text{CH}_3$ ,  $^3J_{\text{HH}} = 7.2$  Hz), 2.11 (m, 2H,  $-\text{CH}_2-\text{CH}$ ), 2.33 (tt, 1H,  $\text{P}-\text{CH}-\text{P}$ ,  $^2J_{\text{PH}} = 24.3$  Hz,  $^3J_{\text{HH}} = 7.1$  Hz), 3.48 (q, 2H,  $\text{N}-\text{CH}_2-$ ,  $^3J_{\text{HH}} = 6.4$  Hz), 3.97 (s, 2H,  $\text{Cl}-\text{CH}_2-$ ), 4.13 (m, 8H,  $\text{O}-\text{CH}_2-$ ), 7.33 (bs, 1H,  $-\text{NH}-$ ).  $^{31}\text{P}$  NMR ( $\text{CDCl}_3$ , 161.9 MHz):  $\delta$  23.7 (m). MS(+): 429.9 (M +  $\text{Na}^+$ ), 445.6 (M +  $\text{K}^+$ ).

**(4-[(Bis(phosphonopropyl)carbamoyl)methyl]-7,10-bis(carboxymethyl)-1,4,7,10-tetraazacyclododec-1-yl)acetic Acid (2b).** Annealed  $\text{K}_2\text{CO}_3$  (5.7 g, 41 mmol) was added to a solution of  $t\text{-Bu}_3\text{DO}_3\text{A}\cdot\text{HBr}$  (4.92 g, 8.2 mmol) in dry acetonitrile (250 mL). Then, a solution of bis(phosphonate) (**7**; 3.37 g, 8.3 mmol) in dry acetonitrile (50 mL) was added in one portion. The mixture was stirred for 4 d at RT and monitored by  $^{31}\text{P}$  NMR spectroscopy. After treatment with charcoal and filtration, the solvents were evaporated off under vacuum. The resulting oil was hydrolyzed in two steps. First the  $t$ -butylester groups were removed by refluxing with a mixture of  $\text{CF}_3\text{COOH}$  (50 mL) and  $\text{CH}_2\text{Cl}_2$  (50 mL) overnight. Then, after evaporation of the volatile compounds under vacuum, the ethylester groups were hydrolyzed off with HBr (30%) in dry AcOH (200 mL) at RT for 24 h ( $^{31}\text{P}$  NMR monitoring). After evaporation of volatiles, traces of HBr were removed by repetitive coevaporation with  $\text{H}_2\text{O}$ . The resulting orange oil was purified on a strong cation exchange resin (Dowex 50, 100/50 mesh, Fluka, elution with water followed by 10% aqueous pyridine). The final purification was performed by repeated column chromatography on a weak cation exchange resin (Amberlite CG 50, Fluka, 600 mL, elution with  $\text{H}_2\text{O}$ , 100 mL fractions). The pure product, which was eluted in the very first fractions, was precipitated by slowly dropping an aqueous solution of it (50 mL) into anhydrous EtOH (400 mL). The precipitate was filtered off, washed with EtOH, and dried over  $\text{P}_2\text{O}_5$ . Yield 1.5 g (30%) of a white powder. Anal. ( $\text{C}_{19}\text{H}_{37}\text{N}_5\text{O}_{13}\text{P}_2\cdot 5\text{H}_2\text{O}$ ) C, H, N.  $^1\text{H}$  NMR ( $\text{D}_2\text{O}$ ,  $90^\circ\text{C}$ , pH = 2.4, 400 MHz):  $\delta$  2.12 (m, 2H,  $-\text{CH}_2-\text{CH}-\text{P}$ ), 2.40 (tt, 1H,  $\text{P}-\text{CH}-\text{P}$ ,  $^2J_{\text{PH}} = 23.1$  Hz,  $^3J_{\text{HH}} = 6.8$  Hz), 3.30 (bs, 8H,  $-\text{CH}_2-\text{N}$ -pendant), 3.33 (bs, 4H,  $-\text{CH}_2-\text{N}$ -pendant), 3.35 (bs, 4H,  $-\text{CH}_2-\text{N}$ -pendant), 3.46 (t, 2H,  $\text{CO}-\text{NH}-\text{CH}_2-$ ,  $^3J_{\text{HH}} = 6.8$  Hz), 3.76 (s, 2H,  $-\text{CH}_2-\text{CO}$ ), 3.79 (s, 2H,  $-\text{CH}_2-\text{CO}$ ), 3.84 (s, 4H,  $-\text{CH}_2-\text{COOH}$ ).  $^{13}\text{C}\{^1\text{H}\}$  NMR ( $\text{D}_2\text{O}$ ,  $25^\circ\text{C}$ , pH = 2.4, 100.6 MHz): 27.08 (bs, 1C,  $-\text{CH}_2-\text{CH}-\text{P}$ ), 37.7 (t, 1C,  $\text{P}-\text{CH}-\text{P}$ ,  $^1J_{\text{PC}} = 121.5$  Hz), 41.08 (t, 1C,  $-\text{CH}_2-\text{CH}_2-\text{CH}-\text{P}$ ,  $^3J_{\text{PC}} = 14.4$  Hz), 52.45 (bs, 8C,  $-\text{CH}_2-\text{N}$ -pendant), 56.5 (bs, 3C,  $-\text{CH}_2-\text{CO}$ ), 58.09 (bs, 1C,  $-\text{CH}_2-\text{CO}$ ), 173.50 (bs, 4C,  $-\text{CO}-$ ).  $^{13}\text{C}\{^1\text{H}\}$  NMR ( $\text{D}_2\text{O}$ ,  $90^\circ\text{C}$ , pH = 2.4, 100.6 MHz): 26.14 (bs, 1C,  $-\text{CH}_2-\text{CH}-\text{P}$ ), 37.9 (bs, 1C,  $\text{P}-\text{CH}-\text{P}$ ), 40.30 (bs, 1C,  $-\text{CH}_2-\text{CH}_2-\text{CH}-\text{P}$ ), 52.24 (bs, 2C,  $-\text{CH}_2-\text{N}$ -pendant), 52.41 (bs, 2C,  $-\text{CH}_2-\text{N}$ -pendant), 52.62 (bs, 2C,  $-\text{CH}_2-\text{N}$ -pendant), 52.82 (bs, 2C,  $-\text{CH}_2-\text{N}$ -pendant), 56.89 (bs, 1C,  $-\text{CH}_2-\text{CO}$ ), 57.00 (bs, 2C,  $-\text{CH}_2-\text{CO}$ ), 58.09 (bs, 1C,  $-\text{CH}_2-\text{CO}$ ), 171.21 (s, 1C,  $-\text{CO}-$ ), 173.39 (s, 2C,

$-\text{CO}-$ ), 174.54 (s, 1C,  $-\text{CO}-$ ).  $^{31}\text{P}$  NMR ( $\text{D}_2\text{O}$ ,  $90^\circ\text{C}$ , pH = 2.4, 161.9 MHz):  $\delta$  24.9 (m). MS(+): 606.6 (M +  $\text{H}^+$ ), 627.9 (M +  $\text{Na}^+$ ), 644.6 (M +  $\text{K}^+$ ). MS(-): 604.2 (M -  $\text{H}^+$ ).

**Preparation of the Ln(III) Complexes.** The ligand **2b** was dissolved in  $\text{H}_2\text{O}$  and the pH was adjusted to 8–9 by an aqueous solution of NaOH (20%). Then, an aqueous solution of hydrated Ln(III) chloride or nitrate (0.9 equiv) was added, and the mixture was heated at  $80^\circ\text{C}$  overnight. The complexation was monitored by  $^{31}\text{P}$  NMR. The procedure for preparation of Ln(III) complexes of **2a** has been published elsewhere.<sup>15</sup> Neither Chelex resin for removing of free Ln(III) ions nor xylenol orange for detection of free Ln(III) ions could be used in the presence of the strongly chelating bis(phosphonates). Therefore, Ln(III) complexes with 10% excess of free ligand were used to avoid the presence of free metal ions.

**Preparation of Radioactive Complexes for Animal Studies.** Lu-**2a** and Lu-**2b**, containing radionuclide  $^{177}\text{Lu}$ , were prepared by mixing 50–400  $\mu\text{L}$  of an aqueous solution containing 200 or 600  $\mu\text{g}$  of the bis(phosphonate) ligand under study with 15–20  $\mu\text{L}$  1 M NaOH and 15–20  $\mu\text{L}$  of an aqueous solution of  $^{177}\text{LuCl}_3$  (75–80 MBq  $^{177}\text{Lu}$ , specific activity 740 MBq  $^{177}\text{Lu}/\mu\text{g}$  Lu) at pH 9 at  $80^\circ\text{C}$  for 90 min. An  $^1\text{H}$  NMR analysis of a sample of the corresponding (nonradioactive) Yb-complex, prepared under similar conditions showed that the metal ion was fully complexed. In vivo experiments were performed in the presence of DTPA in a 100 molar excess of free ligand with respect to the metal ion, as described earlier.<sup>35,36</sup>

**Relaxometric Study of Gd-2b Adsorbed on HA.** HA (1.0 g) was suspended in 5 mL of a 4.2 mM solution of Gd-**2b** in TRIS buffer solution (0.10 M) at pH 7.5. The suspension was shaken gently for 3 d at RT. After sedimentation (2 h) in an NMR tube, the volume ratio of the supernatant to slurry was about 1:1. The supernatant was removed carefully, and the  $^1\text{H}$  NMRD profile of the remaining slurry was measured. The diamagnetic contribution of HA and TRIS buffer to  $R_1$  was subtracted from the data obtained (see Results and Discussion). The concentration of Gd-**2b** in the HA slurry was 8.4 mM.

**Animal Experiments.** Male Lewis rats (250 g) were kept under standard laboratory conditions (12 h light/12 h dark) and were given standard laboratory diet and water ad libitum. The pharmacokinetics were studied by injecting 75–80 MBq of a solution of the  $^{177}\text{Lu}$ -complex (specific activity 740 MBq  $^{177}\text{Lu}/\mu\text{g}$  Lu), containing a total amount of 200 or 600  $\mu\text{g}$  of the bone targeting ligand (**2a** or **2b**) in the penis vein. For comparison, a similar experiment was performed with  $^{177}\text{Lu-3}$  and  $^{177}\text{LuCl}_3$ .<sup>35</sup> The radiolabeled complexes were prepared by mixing aqueous solutions with saline. The distribution of the radiolabel was studied in vivo by  $\gamma$ -camera scintigraphy (Rota II-Siemens, Germany) and by a Nanospect SPECT/CT imager. Biodistributions were determined as described previously.<sup>35</sup> Animals were kept, treated, and cared for in accordance with Erasmus MC animal welfare guidelines.

**Acknowledgment.** We are very grateful to R. Blangé, E. de Blois, and M. Bijster of the Erasmus MC in Rotterdam, The Netherlands, for performing the in vivo experiments. Thanks are due to the EU for financial support via a Marie Curie Early Stage Training fellowship (MEST-CT-2004-7442), to the Grant Agency of the Czech Republic (No. 203/03/0168), to the Long Term Research Plan of the Ministry of Education of the Czech Republic (No. MSM0021620857), and Academy of Science of the Czech Republic (No. KAN201110651, program “Nanotechnology for Society”). This work was done in the frame of COST Action D38 “Metal-Based Systems for Molecular Imaging Applications” and the EU Network of Excellence European Molecular Imaging Laboratory” (EMIL, LSCH-2004-503569).

**Supporting Information Available:**  $^1\text{H}$  NMR spectra of Eu-**2b** and Yb-**2b** complexes, model of molecular structure of  $[\text{Yb}(\text{H}_2\text{O})(\text{H}2\text{b})]^{3+}$ , NMR titration curves of Yb-**2a** and of Yb-**2b**,  $^1\text{H}$  NMRD and  $^{17}\text{O}$  NMR data and a full list of best fit parameters,



SPECT/CT image of Lewis rats 1 h after injection of  $^{177}\text{Lu-2a}$  and  $^{177}\text{Lu-2b}$ , ex vivo radiographs of the femur of Lewis rat 24 h after injection of  $^{177}\text{Lu-2a}$  and  $^{177}\text{Lu-2b}$ , ex vivo radiographs of kidneys of Lewis rat 24 h after injection of  $^{177}\text{LuCl}_3$ ,  $^{177}\text{Lu-3}$ , and  $^{177}\text{Lu-2a}$ , or  $^{177}\text{Lu-2b}$ , and elemental analyses of compounds **2a** and **2b**. This material is available free of charge via the Internet at <http://pubs.acs.org>.

## References

- (1) Merbach, A. E.; Tóth, E. Eds. *The chemistry of contrast agents in medical magnetic resonance imaging*; John Wiley and Sons: Chichester, 2001.
- (2) Caravan, P.; Ellison, J. J.; McMurry, T. J.; Laufer, R. B. Gadolinium(III) chelates as MRI contrast agents: Structure, dynamics, and applications. *Chem. Rev.* **1999**, *99*, 2293–2352.
- (3) Jacques, V.; Desreux, J. F. New classes of MRI contrast agents. *Top. Curr. Chem.* **2002**, *221*, 123–164.
- (4) Aime, S.; Geninatti Crich, S.; Gianolio, E.; Giovenzana, G. B.; Tei, L.; Terreno, E. High sensitivity lanthanide(III) based probes for MR-medical imaging. *Coord. Chem. Rev.* **2006**, *250*, 562–1579.
- (5) Bagi, C. M. Targeting of therapeutic agents to bone to treat metastatic cancer. *Adv. Drug Delivery Rev.* **2005**, *57*, 995–1010.
- (6) Adzamlı, I. K.; Gries, H.; Johnson, D.; Blau, M. Development of phosphonate derivatives of gadolinium chelates for NMR imaging of calcified soft tissues. *J. Med. Chem.* **1989**, *32*, 139–144.
- (7) Schwochau, K. *Technetium chemistry and radiopharmaceutical applications*. Wiley-VCH: Weinheim, Germany, 2000.
- (8) Fleisch, H. *Bisphosphonates in bone disease*. Academic Press: London, UK, 2000.
- (9) Alves, F. C.; Donato, P.; Sherry, A. D.; Zaheer, A.; Zhang, S.; Lubag, A. J. M.; Merritt, M. E.; Lenkinski, R. E.; Frangioni, J. V.; Neves, M.; Prata, M. I. M.; Santos, A. C.; de Lima, J. J. P.; Geraldes, C. F. G. C. Silencing of phosphonate-gadolinium magnetic resonance imaging contrast by hydroxyapatite binding. *Invest. Radiol.* **2003**, *38*, 750–760.
- (10) Bligh, S. W. A.; Harding, C. T.; McEwen, A. B.; Adler, P. J.; Kelly, J. D.; Marriott, J. A. Synthesis, characterization and comparative study of aminophosphonate chelates of gadolinium(III) ions as magnetic resonance imaging contrast agents. *Polyhedron* **1994**, *13*, 1937–1943.
- (11) Adzamlı, I. K.; Johnson, D.; Blau, M. Phosphonate-modified GdDTPA complexes II. Evaluation in a rat myocardial infarct model. *Invest. Radiol.* **1991**, *26*, 143–148.
- (12) Adzamlı, I. K.; Blau, M. Phosphonate-modified GdDTPA complexes I. NMRD study of the solution behavior of new tissue-specific contrast agents. *Magn. Reson. Med.* **1991**, *17*, 141–148.
- (13) Adzamlı, I. K.; Blau, M.; Pfeffer, M. A.; Davis, M. A. Phosphonate-modified GdDTPA complexes. III. The detection of myocardial infarction by MRI. *Magn. Reson. Med.* **1993**, *29*, 505–511.
- (14) Greb, W.; Blum, M.; Roth, M. Contrast medium for using in image-producing methods. PCT WO 03/097074, 2003.
- (15) Kubíček, V.; Rudovský, J.; Kotek, J.; Hermann, P.; Vander Elst, L.; Müller, R. N.; Kolar, Z. I.; Wolterbeek, H. T.; Peters, J. A.; Lukeš, I. A. Bisphosphonate monoamide analogue of DOTA: A potential agent for bone targeting. *J. Am. Chem. Soc.* **2005**, *127*, 16477–16485.
- (16) Vitha, T.; Kubíček, V.; Hermann, P.; Kolar, Z. I.; Wolterbeek, H. T.; Peters, J. A.; Lukeš, I. Complexes of DOTA-bisphosphonate conjugates—Probes for determination of adsorption capacity and affinity constants of hydroxyapatite. *Langmuir*, in press.
- (17) Aime, S.; Botta, M.; Fasano, M.; Marques, M. P. M.; Geraldes, C. F. G. C.; Pubanz, D.; Merbach, A. E. Conformational and coordination equilibria on DOTA complexes of lanthanide metal ions in aqueous solution studied by  $^1\text{H-NMR}$  spectroscopy. *Inorg. Chem.* **1997**, *36*, 2059–2068.
- (18) Aime, S.; Botta, M.; Ermondi, G. Paramagnetic water proton relaxation enhancement—from contrast agents in MRI to reagents for quantitative in vitro assays. *Inorg. Chem.* **1992**, *31*, 4291–4299.
- (19) Howard, J. A. K.; Kenwright, A. M.; Moloney, J. M.; Parker, D.; Port, M.; Navet, M.; Rousseau, O.; Woods, M. Structure and dynamics of all of the stereoisomers of europium complexes of tetra(carboxyethyl) derivatives of dota: ring inversion is decoupled from cooperative arm rotation in the RRRR and RRRS isomers. *Chem. Commun.* **1998**, *13*, 1381–1382.
- (20) Bleaney, B. Nuclear magnetic resonance shifts in solution due to lanthanide ions. *J. Magn. Reson.* **1972**, *8*, 91–100.
- (21) Bleaney, B.; Dobson, C. M.; Levine, B. A.; Martin, R. B.; Williams, R. J. P.; Xavier, A. V. Origin of lanthanide nuclear magnetic resonance shifts and their uses. *J. Chem. Soc., Chem. Commun.* **1972**, 791–793.
- (22) Golding, R. M.; Halton, M. P. Theoretical study of the nitrogen-14 and oxygen-17 NMR shifts in lanthanide complexes. *Aust. J. Chem.* **1972**, *25*, 2577–2581.
- (23) Golding, R. M.; Pyykkö, P. Theory of pseudocontact NMR shifts due to lanthanide complexes. *Mol. Phys.* **1973**, *26*, 1389–1396.
- (24) Pinkerton, A. A.; Rossier, M.; Spiliadis, S. Lanthanide-induced contact shifts. The average electron spin polarization, theory and experiment. *J. Magn. Reson.* **1985**, *8*, 420–425.
- (25) Peters, J. A.; Huskens, J.; Raber, D. J. Lanthanide induced shifts and relaxation rate enhancements. *Prog. Nucl. Magn. Reson. Spectrosc.* **1996**, *28*, 283–350.
- (26) Alpoim, M. C.; Urbano, A. M.; Geraldes, C. F. G. C.; Peters, J. A. Determination of the number of inner-sphere water molecules in lanthanide(III) polyaminocarboxylate complexes. *J. Chem. Soc., Dalton Trans.* **1992**, 463–467.
- (27) Djanashvili, K.; Peters, J. A. How to determine the number of inner-sphere water molecules in lanthanide(III)-complexes by  $^{17}\text{O}$  NMR spectroscopy. A technical note. *Contrast Media Mol. Imaging* **2007**, *2*, 67–71.
- (28) Dyba, M.; Kozłowski, H.; Tlalka, A.; Leroux, Y.; El Manouni, D. Oxovanadium(IV) complexes of 1-hydroxyalkane-1,1-diylidiphosphonic acids. *Pol. J. Chem.* **1998**, *72*, 1148–1153.
- (29) Martell, A. E.; Smith, R. M. *Critical stability constants*; Plenum Press: New York, 1974–1989, Vols. 1–6; NIST Standard Reference Database 46 (Critically Selected Stability Constants of Metal Complexes), version 7.0, 2003.
- (30) Kubíček, V.; Kotek, J.; Hermann, P.; Lukeš, I. Aminoalkylbis(phosphonates): their complexation properties in solution and in the solid state. *Eur. J. Inorg. Chem.* **2007**, *2*, 333–344.
- (31) Lebdušková, P.; Kotek, J.; Hermann, P.; Vander Elst, L.; Müller, R. N.; Lukeš, I.; Peters, J. A. A gadolinium(III) complex of a carboxylic-phosphorus acid derivative of diethylenetriamine covalently bound to inulin as a new potential macromolecular MRI contrast agent. *Bioconjugate Chem.* **2004**, *15*, 881–889.
- (32) Powell, D. H.; Dhubghaill, O. M. N.; Pubanz, D.; Helm, L.; Lebedev, Y. S.; Schlaepfer, W.; Merbach, A. E. Structural and dynamic parameters obtained from  $^{17}\text{O}$  NMR, EPR, and NMRD studies of monomeric and dimeric  $\text{Gd}^{3+}$  complexes of interest in magnetic resonance imaging: An integrated and theoretically self-consistent approach. *J. Am. Chem. Soc.* **1996**, *118*, 9333–9346.
- (33) Aime, S.; Botta, M.; Garino, E.; Geninatti Crich, S.; Giovenzana, G.; Pagliarini, R.; Palmisano, G.; Sisti, M. Non-covalent conjugates between cationic polyamino acids and Gd(III) chelates: A route for seeking accumulation of MRI-contrast agents at tumor targeting sites. *Chem.—Eur. J.* **2000**, *6*, 2609–2617.
- (34) Aime, S.; Botta, M.; Fasano, M.; Terreno, E. Lanthanide(III) chelates for NMR biomedical applications. *Chem. Soc. Rev.* **1998**, *27*, 19–29.
- (35) Breeman, W. A. P.; van der Wansem, K.; Bernard, B. F.; van Gameren, A.; Erion, J. L.; Visser, T. J.; Krenning, E. P.; de Jong, M. The addition of DTPA to [ $^{177}\text{Lu-DOTA}^0\text{Tyr}^3$ ]octreotate prior to administration reduces rat skeleton uptake of radioactivity. *Eur. J. Nucl. Med. Mol. Imaging* **2003**, *30*, 312–315.
- (36) Breeman, W. A. P.; de Jong, M. T.; de Blois, E.; Bernard, B. F.; de Jong, M.; Krenning, E. P. Reduction of skeletal accumulation of radioactivity by co-injection of DTPA in [ $^{90}\text{Y-DOTA}^0\text{Tyr}^3$ ]octreotide solutions containing free  $^{90}\text{Y}^{3+}$ . *Nucl. Med. Biol.* **2004**, *31*, 821–824.
- (37) Thakral, C.; Alhariri, J.; Abraham, J. L. Long-term retention of gadolinium in tissues from nephrogenic systemic fibrosis patient after multiple gadolinium-enhanced MRI scans: case report and implications. *Contrast Media Mol. Imaging* **2007**, *2*, 199–205.
- (38) Dadabhoy, A.; Faulkner, S.; Sammes, P. G. Long wavelength sensitizers for europium(III) luminescence based on acridone derivatives. *J. Chem. Soc., Perkin Trans. 2* **2002**, *2*, 348–357.
- (39) Winckler, W.; Pieper, T.; Keppler, B. K. Preparation of octaethyl-3-amino-pentane-1,1,5,5-tetrakisphosphonate by catalytic hydrogenation of the corresponding 3-nitro-compound. *Phosphorus, Sulfur Silicon Relat. Elem.* **1996**, *112*, 137–141.
- (40) Zitha-Bovens, E.; Vander Elst, L.; Müller, R. N.; van Bekkum, H.; Peters, J. A. Relaxivity studies on a gadolinium(III) complex of a macrocyclic DTPA derivative. *Eur. J. Inorg. Chem.* **2001**, *12*, 3101–3105.
- (41) Vold, R. L.; Waugh, J. S.; Klein, M. P.; Phelps, D. E. Measurement of spin relaxation in complex systems. *J. Chem. Phys.* **1968**, *48*, 3831–3832.
- (42) Meiboom, S.; Gill, D. Modified spin-echo method for measuring nuclear relaxation times. *Rev. Sci. Instrum.* **1958**, *29*, 688–691.
- (43) Corsi, D. M.; Platas-Iglesias, C.; van Bekkum, H.; Peters, J. A. Determination of paramagnetic lanthanide(III) concentrations from bulk magnetic susceptibility shifts in NMR spectra. *Magn. Reson. Chem.* **2001**, *39*, 723–726.
- (44) *Scientist for Windows*, version 2.01, Micromath, Inc.: Salt Lake City, UT, 1995.
- (45) Kývala, M.; Lukeš, I. *International Conference Chemometrics '95*, Pardubice, Czech Republic, 1995, p. 63; the full version of OPIUM is available (free of charge) on <http://www.natur.cuni.cz/~kyvala/opium.html>.
- (46) *HyperChem*, Release 7.5 for Windows, Molecular Modeling System, Hypercube, Inc: Ontario, Canada, 2002.